International Forum on Aeroelasticity and Structural Dynamics
IFASD 2024
17-21 June 2024, The Hague, The Netherlands

CONTROL SURFACE SIZING AND DESIGN THROUGH INTEGRATED MDO APPROACH: ENHANCING LOAD ALLEVIATION WHILE PRESERVING HANDLING QUALITIES

Daniel Muradas Odriozola[*1], **Sylvie Marquier**[1], **Joseph Morlier**[2], **Christian Gogu**[2]

[1]Loads and Aeroelastics Engineering,
Airbus Operations SAS,
316 route de Bayonne, 31300 Toulouse,
France

[2]ICA, Université de Toulouse, ISAE-SUPAERO, MINES ALBI, UPS, INSA, CNRS,
3 rue Caroline Aigle, Toulouse, 31400,
France

Keywords: Loads Alleviation, Computational Aeroelasticity, Highly Flexible Aircraft Structures, Aeroelasticity in Conceptual Aircraft Design, Flutter, MDO

Abstract: As part of ongoing efforts for cleaner and more efficient aviation, this research introduces a novel Multidisciplinary Optimisation (MDO) strategy for the weight optimisation of High Aspect Ratio (HAR) wings involving active load alleviation. The study focuses on implementing a Load Alleviation Function (LAF) to reduce wingbox structural loads during manoeuvres or gust encounters by redistributing lift inboard using movable control surfaces [1]. Building upon previous work [2], this MDO process aims to redefine control surface sizing and positioning for an optimised load alleviation while preserving the primary goal of ensuring effective aircraft manoeuvrability. An HAR wing concept is an enabler for enhancing the aircraft overall efficiency, however, it is typically heavier than its lower aspect ratio counterpart. Additionally, it leads to greater flexibility in the wing, directly influencing the efficiency of the control surface and potentially leading to issues such as the control surface reversal phenomena. The challenge thus lies in defining a control surface concept to allow a weight reduction through load alleviation thanks to an optimal position and size of control surfaces, while simultaneously satisfying certification criteria for aircraft manoeuvrability across a diverse set of flight scenarios and ensuring a flutter-free design. To achieve this, an MDO approach is being considered in this work, intended to cover relevant Loads conditions and Handling Quality (HQ) criteria considered for certification such as roll capabilities. The implemented MDO approach considers the following disciplines, static aeroelastic analysis, structural optimisation, flutter constraints, aircraft manoeuvre trimming, handling qualities efficiency assessment, and its associated validation between classic wing concept versus high aspect ratio.

1 INTRODUCTION

The prevailing trend today is to boost civil aviation aircraft efficiency, notably by increasing the wing aspect ratio [3], which enhances the aerodynamic efficiency thanks to a reduction of induced drag. But this improvement comes with a cost and significant structural challenge when increasing the wing span. The first issue to face is that the structure must be able to support what would be a heavier wing compared to a lower aspect ratio design, and, to further increase the span, the trend is to use more flexible, resistant and lightweight materials such as composites [4]. Structures with increased flexibility are prone to dynamic instabilities, such as flutter [5], which diminish the effectiveness of movables. In fact, the deformation of the wing will induce a different apparent angle of attack seen by the aileron. This project aims at developing an MDO framework to get the most benefit of the ailerons design with its most adequate positioning for loads alleviation perspectives while simultaneously ensuring to be flutter free and achieving best aircraft control. The objective will be to improve the load alleviation configuration through the ailerons while ensuring a flutter-free manoeuvrable aircraft. Furthermore, comparing classical and high aspect ratio wing concepts.

The load alleviation (LAF) or manoeuvre load alleviation (MLA) system is a structural load mitigation system that is active during a manoeuvre. There are many ways to achieve load alleviation [6, 7], but for this study only the active load alleviation through movables will be addressed. This system has been in use since its integration in the A320 [8], where a potential net load reduction of 15% was shown at the wing root. This system must still comply with the European Union Safety Agency (EASA) [9] and the Federal Aviation Administration (FAA) [10] in the United States regulations.

The general principle of LAF as considered in this work is to achieve a redistribution of the aerodynamic loading along the span of the wing such as to decrease the bending moment at the root of the wing.The working principle of load alleviation is, while manoeuvring, to further increase the angle of attack of the aircraft which would lead to an increase of loads, but this excess of lift is purposely removed from the wing via a deployment of movables. Effectively, the same load factor is in place, but the load has been redistributed more inboard.

2 THEORETICAL BACKGROUND

This section 2 serves as a brief overview of the disciplines involved in the optimisation process, where the key aspects of each discipline are explored.

2.1 Aeroelastic modelling

Following previous work [2], the aircraft model used is the undeflected common research model (uCRM) [11], a modified version of the common research model by NASA [12]. Given the half-wing model for both short (uCRM9) and long (uCRM135) aspect ratio aircraft models, they were adapted to a full model to better resemble a global finite element model (GFEM), notably including the horizontal tail plane to be able to trim the aircraft in the different set of manoeuvres.

The full model enables a proper evaluation of the flutter response as it will output both symmetric and anti-symmetric modes. Similarly for roll analysis, the complete model enables tracking of asymmetric behavior, which cannot be done through a half wing model. LAF during roll manoeuvres will thus not be considered in this study, but is considered in a line of future work to address the influence of the LAF on the tuning of the control law. The properties of both aircraft are mentioned in table 1 and the GFEM of both models is shown in figure 2.

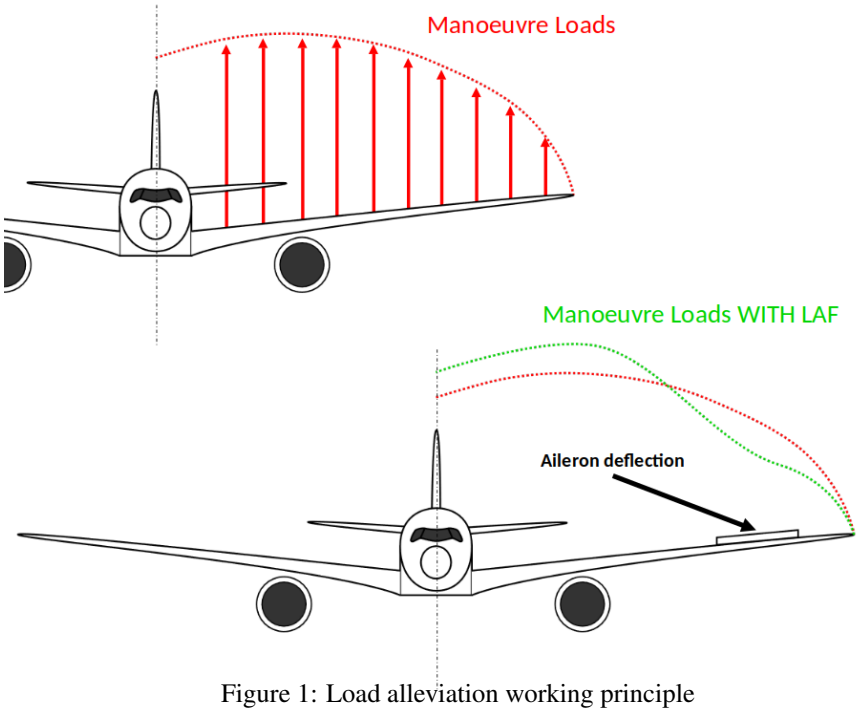

Figure 1: Load alleviation working principle

Table 1: Design properties for both aircraft (A/C).

A/C	uCRM9	uCRM13.5
AR [-]	9	13.5
Span [m]	58.76	72.00
Wing area [m²]	383.638	384
MTOW [ton]	297.5	284.256
MZF [ton]	187.5	185.256
Mach Cruise [-]	0.85	0.85
Cruise alt. [kft]	37	37

The aerodynamic model is created with NASTRAN's CAERO definition, which creates a set of DLM panels for a quick linear aerodynamic load estimation. This method will allow a fast manoeuvre computation with a global trim of the aircraft, although as not as high fidelity as CFD the flight conditions covered within this study are at high angles of attack, which CFD will struggle to converge. So, for now, the simplest approach is to rely on DLM.

To fully address the properties of the aircraft, an additional mass was created to balance the aircraft so that its centre of mass would appear where desired. And the remaining masses due to the fuselage and payload were accounted for there.

The wingbox is defined via a set of flat panels CQUAD4, with a PSHELL definition for its thickness. It will be this value with which the optimiser will play to search for the optimal sizing taking advantage of load alleviation. The wingbox, as considered in [13], is entirely made of Aluminium alloy.

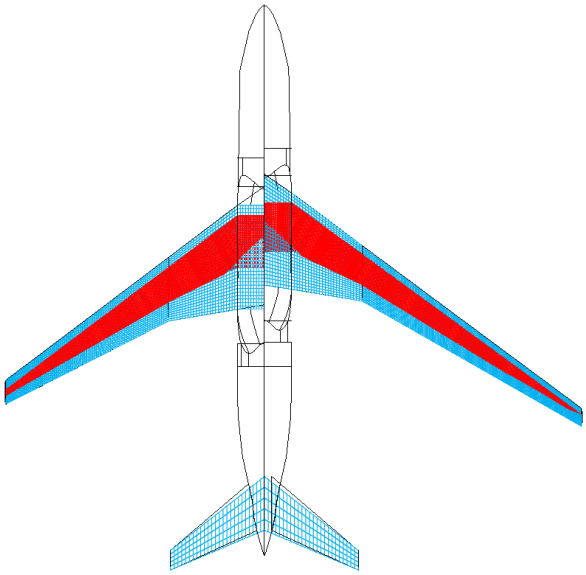

Figure 2: uCRM AR9 Left and uCRM AR13.5 Right

2.2 Aileron Sizing and Loads Optimisation

The method introduced in our previous publication [2] seeking to obtain the optimal placement of the aileron was further improved here. The optimiser present in our previous work consisted of a simple finite-difference method to search for the best aileron placement for minimal wing bending moment.

The aerodynamic definition of the control surfaces involves choosing a set of panels to describe the control surface, and its deflection is set through adjustments to the relative flow boundary conditions of each panel. For this study, the same parametrisation will be employed as in previous works, the position and size of the aileron will be interpolated from a continuous function onto the discrete DLM panels as seen in figure 3.

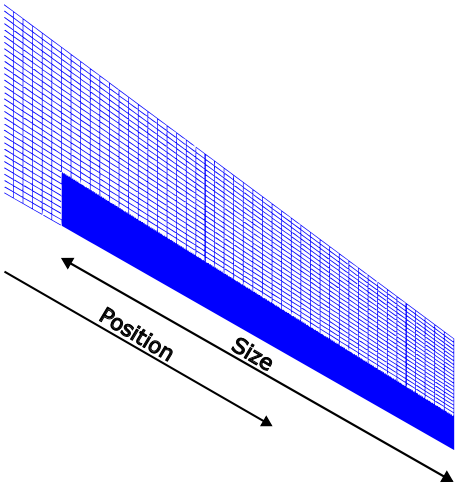

Figure 3: Detail on wingtip DLM panels and aileron parametrisation

This approach requires a method to transform into continuous variables the discrete aerodynamic panels, the aileron size and placement can be represented as a set of aerodynamic panels which can in turn be parameterised for a given span. These parameters will be the design variables during the optimisation process, and this transformation from continuous to discrete

variable will be done ”on the fly” for each iteration, which means that for very high precision values the disciplines might not differentiate between two very close aileron configurations, to fix that a minimum step size is specified which will ensure a proper derivative calculation.

From the results of [2] it was concluded that an inboard aileron placement would improve the load alleviation. The total size of the aileron will tend to the maximum allowed, this is due to the use of a linear aerodynamic solver, which means the greater the surface area the more efficient it will become in load alleviation with no penalty due to flow separation, and it is the same for the aileron deflection angle. Also, it is worth mentioning that a decisive factor for aileron sizing is the capabilities of the actuators used, so both the area and the deflection are constrained by their total force exerted and responsiveness. To further build on the MDO architecture the interest now is to see what improvements in performance can be achieved via structural mass reduction thanks to a new sizing of the wing-box.

2.3 Structural sizing

As briefly introduced in section 2.1 the structure consists of a series of shell panels with a given thickness defining the wingbox. This thickness will be the design variable for the structural sizing, and there are a total of 242 thickness design variables for the uCRM9 and 287 for the uCRM135.

The sizing of the structure is performed through solution 200 of NASTRAN, which for a given set of flight maneuvers will adjust the thickness of each structural panel within the stress constraints to reduce the structural aircraft mass. Furthermore, to take into account aero-structural dynamic effects, a flutter constraint is included, which will be explained in more detail in Section 2.5.

The structural sizing itself is an optimisation process that evaluates the sensitivities of each design variable to the redesign of the structure that better suits the objective and its constraints. In the Nastran’s Design Sensitivity and Optimisation User’s Guide [14] it is further explained how this process works.

The structural constraints are rather simple, to avoid having to set a wing deformation constraint that would limit the flexibility of the wing, a stress constraint is included similarly to what was done in other works such as [15, 16]. More freedom is allowed for the wing deformation, and as a yield stress reference, a 2.5g maneuver was performed with the baseline configuration and its stress values were extracted; the von Mises stress maxima was selected as reference for the optimisation.

The rationale behind selecting the maximum von Mises stress observed during the baseline 2.5g manoeuvre as the stress constraint, rather than using the material yield stress, is due to the fact that the baseline models did not satisfy the maximum yield stress of 420MPa for aluminium. In contrast, other studies, like [13], incorporate more comprehensive stress constraints, including buckling considerations and various solvers. Instead of undergoing extensive design alterations, it was opted for a simpler stress constraint approach.

Finally to create a fair comparison, the structure was resized with the constraints mentioned above for the same manoeuvre flight conditions, but this time without load alleviation active. The objective was to create a new baseline configuration, and when comparing with the results of the sizing process with MLA active, all mass optimizations would exclusively originate

from load alleviation. This new baseline will preserve the same flutter properties and stress properties.

2.4 Estimation of roll capabilities

The handling qualities aspect (HQ) of an aircraft is a difficult discipline to properly evaluate at early stages of design. For conceptual aircraft design, there are no specific rules to follow; the aircraft must be manoeuvrable, that is, it must be able to be safely controlled in very different sets of conditions. The EASA certification specifications for large aircraft CS-25 [9] have some rules that every commercial aircraft must follow. Some of which involving aileron sizing are:

- CS 25.147(f): "*Lateral control; all engines operating. With the engines operating, roll response must allow normal manoeuvres (such as recovery from upsets produced by gusts and the initiation of evasive manoeuvres). There must be enough excess lateral control in sideslips (up to sideslip angles that might be required in normal operation), to allow a limited amount of manoeuvring and to correct for gusts. Lateral control must be enough at any speed up to VFC/MFC to provide a peak roll rate necessary for safety, without excessive control forces or travel.*"

And as mentioned in the Acceptable Means of Compliance (AMC) for the CS 25.147(f): "*An acceptable method of demonstrating that roll response and peak roll rates are adequate for compliance with CS 25.147(f) is as follows: It should be possible in the conditions specified below to roll the aeroplane from a steady 30° banked turn through an angle of 60° so as to reverse the direction of the turn in not more than 7 seconds. In these demonstrations, the rudder may be used to the extent necessary to minimise sideslip.*"

Although this AMC seems very specific and it might play a very important role for the aileron sizing and positioning, it does not specify which control surfaces should be used to perform said manoeuvre, and it does not specify if you need to use control surfaces to perform the turn. Additionally, a simple static aeroelastic computation that lacks a control law cannot determine the total bank turn time required in CS 25.147(f).

Other specific AMCs such as AMC 25.147(d) go even further and specify the turn conditions with some inoperative engines to ensure the aircraft is still manoeuvrable during failure cases, but at this current stages and also for this specific study case there is no data for engine performance.

For this reason, a simpler approach must be conceived to ensure acceptable handling qualities. From experience, in the early stages of the design, the approach is to set a target roll acceleration that must be achieved with only the ailerons, although additional control surfaces such as spoilers are participating in the roll efficiency, but not considered in this analysis, nevertheless it makes it a more conservative approach. This can be computed within a static analysis and it can give an insight on the roll performance, for this case a roll acceleration of 7°/s² was selected for this long-range-like aircraft.

Now that the target roll rate has been defined, the next step is to define the flight conditions. To find the most critical cases we must refer to the equation of motion for roll acceleration:

$$\dot{p} = \frac{\bar{q} S l C_{l\delta_p} \delta_p}{I_{xx}} \tag{1}$$

Where $\dot{p}$ is the roll acceleration, $\bar{q}$, S, $C_{l\delta p}$, δ_p and I_{xx} are the dynamic pressure, surface area, lift coefficient, and moment of inertia on x or roll moment of inertia, respectively.

The most critical scenario, in this case it is the condition for which the aileron is subjected to the greatest deflection angle possible. Following equation 1, for a given roll acceleration $\dot{p}$, the critical case is found during low-speed manoeuvres involving low dynamic pressures $\bar{q}$. This would be the case of a landing approach and it will also be the scenario in which the aircraft needs to target a precise descent path, requiring immediate responses from the controls to adapt to the wind changes.

Finally, roll capability will be defined as the inverse of trim aileron angle deflection for a given roll rate divided by the maximum allowable aileron deflection. That is:

$$\text{roll capability margin} = \left[\frac{\text{aileron deflection}(\dot{p} = 7^\circ/s^2)}{\text{max aileron deflection}}\right]^{-1} \tag{2}$$

This means that the aileron roll margin will drop below 100% when the aileron deflection is greater than the maximum possible.

2.5 Flutter modeling

Flutter is a structural dynamic instability of an elastic structure in a fluid flow, caused by a positive feedback between the body deflection and the force exerted by the fluid flow. The end goal is to track the evolution of the damping for several flight speeds. Following NASTRAN notation, the negative damping is stable. In this case there is no record that neither the uCRM9 or uCRM135 were sized with flutter in mind. Nevertheless its integration in the design process is important for certification process, a constraint for a valid design needs to be imposed, in this case the design must be flutter free up to 1.15 times the dive speed (see EASA Certification regulation CS 25.629 [9]).

In order to properly introduce the flutter optimisation, the solver must be capable of computing the design variables sensitivities. Nastran achieves this via solving the eigenvalue problem for flutter [17] given by equation 3. It uses the PK-flutter analysis [18], which is more convenient for this use case as it will perform the analysis for a given set of velocities.

$$\left[M_{hh}p^2 + \left(B_{hh} - \frac{1}{4}\rho\bar{c}VQ^I_{hh}/k\right)p + \left(K_{hh} - \frac{1}{2}\rho V^2 Q^R_{hh}\right)\right]\{u_h\} = 0 \tag{3}$$

Where M_{hh}, B_{hh} and K_{hh} are the generalised mass, damping and stiffness matrices, respectively. And Q_{hh} is the complex modal aerodynamic damping matrix as a function of the mach number and reduced frequency k, which is divided in real Q^R_{hh} and Q^I_{hh} imaginary part. u_{hh} would be the displacement vector. ρ, $\bar{c}$ and V are the density, chord and velocity.

p is the complex eigenvalue $p = \omega(\gamma + i)$, composed of the frequency ω and the transient decay γ. The damping coefficient is then $g = 2\gamma$. To address flutter instabilities, Nastran calculates the sensitivities for each design variable with respect to γ.

An issue comes with what is called mode tracking, the structure has many modes that change frequency with the speed and their damping curves might cross each other which might lead

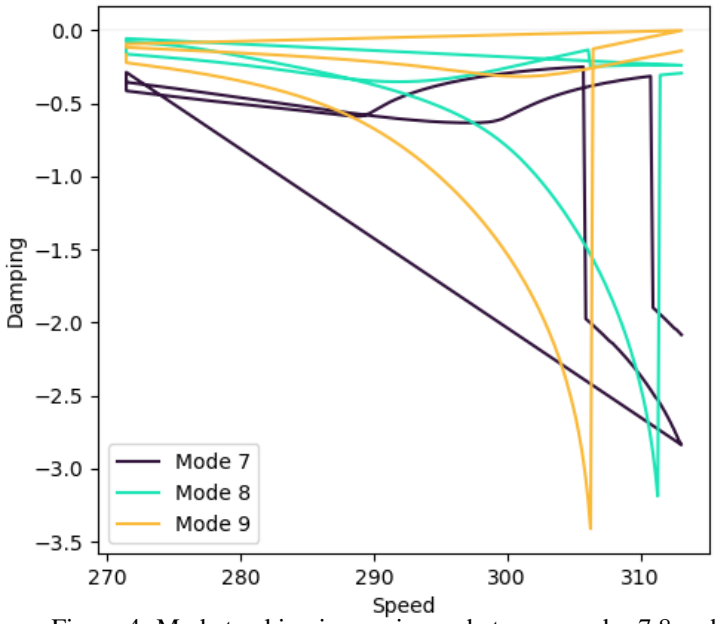

Figure 4: Mode tracking issues, jumps between modes 7,8 and 9

to discontinuities within the sensitivity analysis. This phenomena is extensively explained in [19, 20] where great effort has been done to further improve the gradient computation for flutter analysis. However, for this simple approach the Nastran solution was used as a preliminary approach.

As can be seen in figure 4 sometimes jumps in between modes occur leading to discontinuities in the sensitivity analysis.

3 PROBLEM DESCRIPTION

To adequately establish the optimisation problem, the objective can be defined as follows:

$$
\begin{aligned}
\text{Minimize} \quad & Mass(\text{pos})_i \\
& \text{Max}(Mx(\text{pos})_i) \\
\text{w.r.t.} \quad & \text{pos} \\
\text{subject to} \quad & Stress(\text{pos}) < Reference\ stress\ @\ 2.5g \\
& Roll\ Capability(\text{pos}) > 100\% \\
& Flutter\ Speed(\text{pos}) > 1.15V_d \approx 313m/s
\end{aligned}
\tag{4}
$$

Where pos is the position of the aileron, $Mass(\text{pos})$ is the wingbox mass obtained from a sizing process for a given aileron position and it is the main objective, and $\text{Max}(Mx(\text{pos})_i)$ is the maximum wing bending moment found in the set of sizing manoeuvres for a given aileron position. The stress, following the von Mises stress criterion, must not be superior to a reference value found in a 2.5 g manoeuvre for the baseline configuration. Roll capabilities must always be within the manoeuvrability margins, i.e. above 100%, and finally, the flutter speeds must not exceed $1.15V_d$ as required by regulations [9].

4 OPTIMISATION PROCESS

Now that all disciplines have been presented, the optimisation process must be defined. The interest of this paper is to evaluate different approaches to solve the optimisation problem with the tools available. Two different approaches were created with the same objective, and to further comprehend the process, it was staggered in several steps.

This section will start with a detailed description through sections 4.1, 4.2, 4.3 and 4.4, where two possible MDO architectures will be presented. Then in sections 5.1 and 5.2 the results for the same architectures will be discussed, for both low- and high-aspect ratio models (uCRM9 and uCRM13.5).

4.1 Bending moment optimisation

This optimisation step was already proposed in the previous publication [2] and will be the basis for the complete optimisation. Thanks to this approach, it was shown that it is possible to further reduce wing bending loads through an inboard repositioning of the aileron. The flowchart is presented in figure 5 and consists of a finite-difference Sequential Least Squares Programming (SLSQP) optimiser coupled on top of the NASTRAN Manoeuvre MDA discipline, in which the static aeroelastic problem with trim is solved. It is handled by GEMSEO, a Generic Engine for Multidisciplinary Scenarios, Exploration and Optimisation [21].

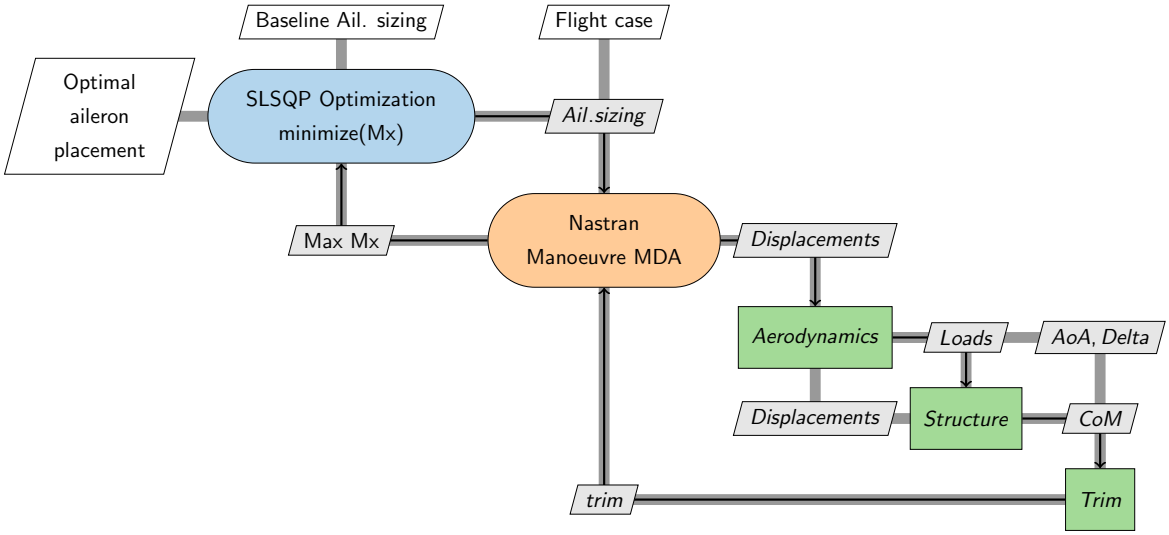

Figure 5: Wing bending optimisation via aileron resizing

The eXtended design Structure Matrix (XDSM) [22] presented in figure 5 shows the data flow within disciplines, where aileron sizing properties (Ail. sizing.) such as aileron position, serve as the main design variable input to feed the optimiser to find the minimum bending moment possible. The main process is the static aeroelastic Multi Disciplinary Analysis (MDA), which, given a GFEM, computes the loads loop. Starting with aerodynamics (Aero.), the loads are computed serving as input for the structural discipline (Struct.), to derive the structural wing displacements (Displ.) which would change the aerodynamic loads, restarting this process. Once this loop has converged, the next step is to trim the aircraft, it is another iterative process for finding the required flight trim variables such as the angle of attack (AoA) and horizontal tail

plane deflection (delta) necessary to reach equilibrium in a given manoeuvre. Following this, the loads, particularly the wing bending moment, are extracted to feed back to the optimiser.

This optimisation process leads to the results in table 2 for the low aspect ratio wing (uCRM9).

Table 2: Wing bending optimisation via aileron resizing results (AR9)

	Baseline	Optima #1
Aileron size / span [-]	0.3	0.3
Aileron position / span [-]	0.8	0.68
Aileron deflection [deg]	15°	15°
Max Mx Bending [Nm]	1.71×10^7	1.66×10^7 (-3%)

In this case the optimisation uses constant aileron size and deflection, as linear aerodynamics will not penalise great aileron deflections or sizes due to flow separation, so in this case there is no need to include them as design variables. However, it has been shown that another 3% load reduction is attainable thanks to inboard repositioning, and, as such, the next step is to study the mass benefit that this allows.

4.2 Mass optimisation based on bending loads optimisation

Parting from the previous process, now the interest lies in coupling a structural sizing solver. Nastran SOL200 will be used, as it will compute the design sensitivities with respect to the objective, in this case mass reduction.

The change in structural mass leads to a change in loads, as the aircraft wings no longer need to sustain the same amount of weight, that is the reason why the structural resizing will lead to a change in the aerodynamics and thus a change in the aileron load alleviation.

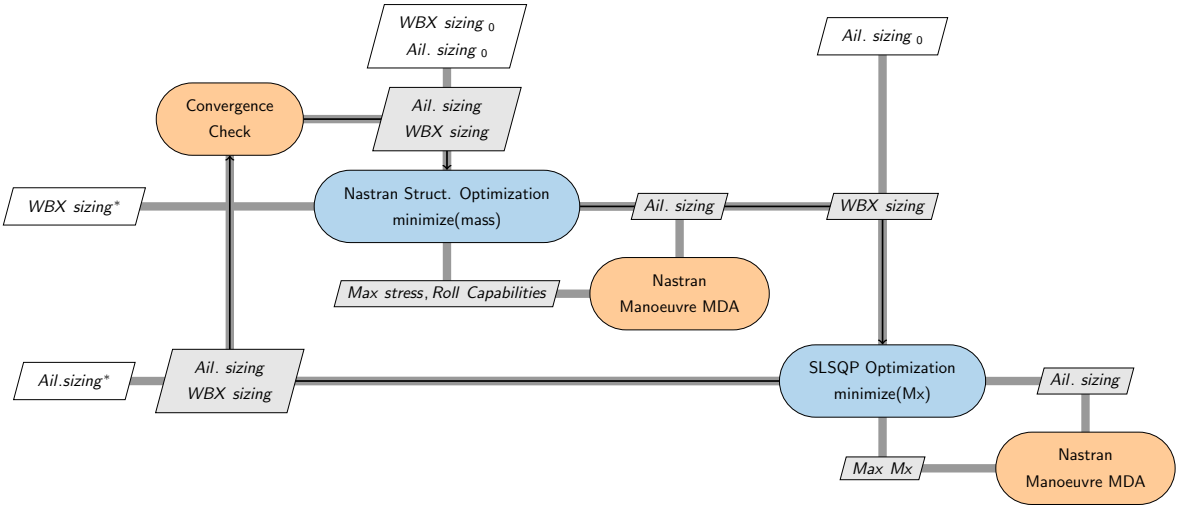

Figure 6: Mass - Wing bending optimisation via aileron resizing

In figure 6 the XDSM is presented, it connects the aircraft GFEM as a blind input to the SLSQP optimiser and from it the aileron design properties become the input for the structural sizing

process. This algorithm will exchange the updated structural and aileron definitions between the two optimisers until convergence is achieved, in this case through a check if the aileron position is changing from two consecutive iterations.

In this case the sizing step will also contain some exclusive constraints, stress and roll capabilities. The respective sensitivities will be automatically computed by Nastran to restrict the optimisation to a feasible design.

4.3 Mass optimisation based on bending loads optimisation with flutter constraint

Clearly, the optimisation process presented in section 4.2 does not consider a flutter constraint, making flutter a likely consequence. As stated in section 2.5 in order to be considered flutter-free the aircraft must not become positively damped below an extra 15% over Dive speed (1.15% Vd), as requested in the regulation CS25.629 - Aeroelastic stability requirements [9]. For this aircraft, the selected speed is roughly around 313 m/s. The first mode to be triggered below this speed is number 15, at 304m/s.

The last step then would be to introduce the flutter constraint, following the flowchart 6, now with flutter constraint inside the structural sizing step. Figure 7 shows the updated XDSM.

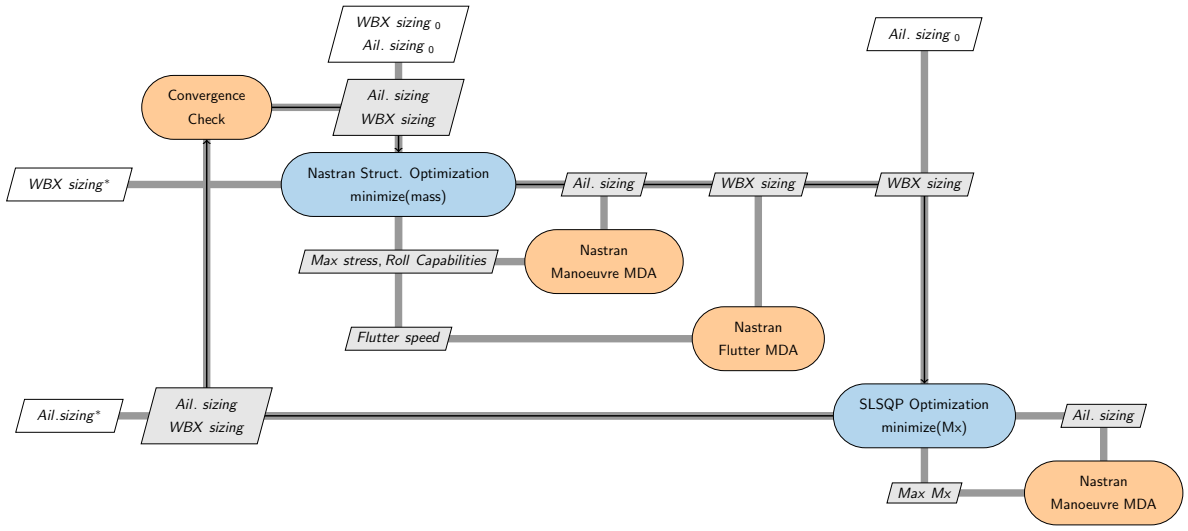

Figure 7: Mass - Wing bending optimisation via aileron resizing with flutter constraint

4.4 Direct mass optimisation

An alternative approach could just consist of a mass optimisation, given that the capabilities of NASTRAN allow parallel execution of both static aeroelastic analysis and flutter for a given FEM. This allows for a simple optimisation test case where a simple finite-difference optimisation process could enclose the Sol200 to try to find the best aileron sizing. The Python optimisation script that contains the NASTRAN Sol200 structural sizing step. With this approach the flight loads do not play any direct role in the optimisation process as they are in theory already taken into account with the stress constraints.

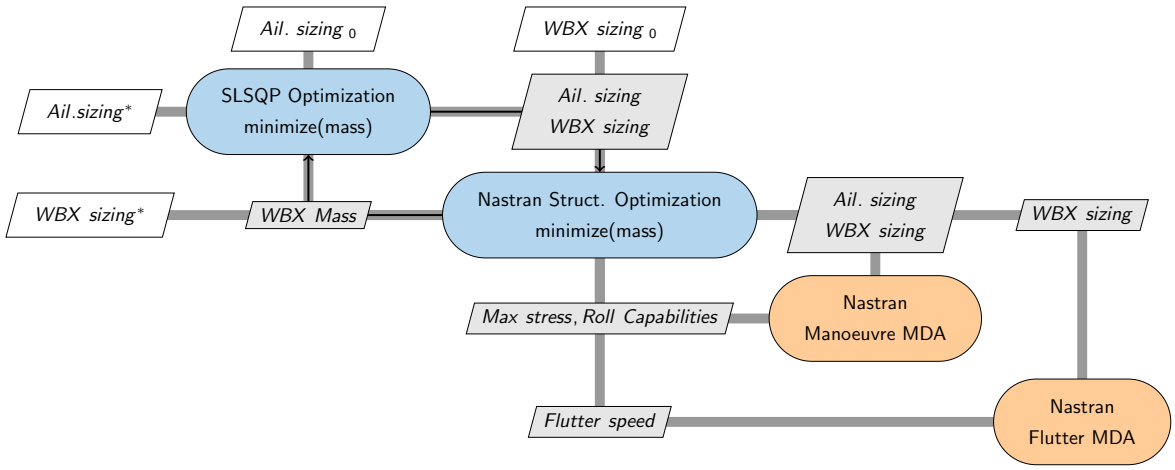

Figure 8: Mass optimisation via aileron resizing with flutter constraint

5 RESULTS AND DISCUSSIONS

5.1 Results for low aspect ratio

Starting from the architecture presented in section 4.2, wingbox structural optimisation through wing bending loads, the uCRM9 model leads to the results in table 3.

Table 3: Mass - Wing bending optimisation via aileron resizing results (uCRM9)

	Baseline	Optima #2
Aileron position / span [-]	0.8	0.633
Max Mx Bending [Nm]	1.71×10^7	1.66×10^7
Structural mass [Ton]	14.702	12.551 (-14.6%)
Roll capability	175.1%	187.5%
Run time [h:min]		00:56

These results show great potential, with a decrease in wing mass by 14% as shown in table 3 and without an important change in roll capabilities.

The mass reduction leads to a stiffness reduction, so it may be relevant to analyse the impact it might have on flutter. Indeed a change of stiffness induces a change in the structural dynamic behaviour . With this new sizing #2, when performing a flutter analysis it leads to the following results shown in figure 9.

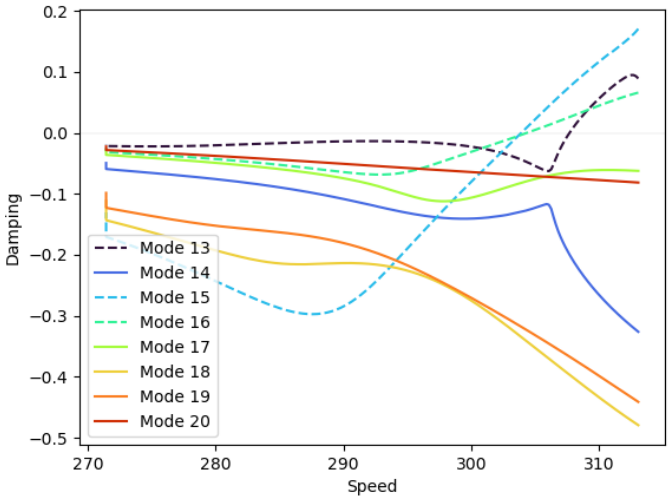

Figure 9: V-g plot for wing from optimisation #2

Obviously, this optimisation process did not take into account a flutter constraint, so it is inherent that flutter could be a possible outcome. As stated in section 2.5 in order to be considered flutter-free the aircraft must not become positively damped below an extra 15% over Dive speed (1.15% Vd), as requested in the regulation CS25.629 - Aeroelastic stability requirements [9]. For this aircraft, the selected speed is roughly around 313 m/s. The first mode to be triggered below this speed is number 15, at 304m/s.

Table 4: Mass - Wing bending optimisation via aileron resizing results (uCRM9)

	Baseline	Optima #2	Optima #3
Aileron position / span [-]	0.8	0.633	0.643
Max Mx Bending [Nm]	1.71×10^7	1.66×10^7	1.65×10^7
Structural mass [Ton]	14.702	12.551 (-14.6%)	13.055 (-11.2%)
Flutter speed [m/s]	>313	303.9	312.545
Roll capability	175.1%	187.5%	186.9%
Run time [h:min]		00:56	01:06

With the approach presented in section 4.3, the mass optimisation based on wing bending loads with flutter constraint, the results from table 4 show, as expected, an improvement in flutter. The optimiser has obtained a design that exactly triggers an instability at around 313m/s. This result of course comes with a drawback in weight, due to the new requirement the design has to be stiffer and thus the structure must be reinforced, but it still results in an 11% wing structural mass reduction. The roll capability has not been really affected, as the aileron position has not changed much, and given that optima #3 is a stiffer structure, the optimal position lies more outboard.

Finally, in table 5 the two complete approaches are compared, with both cases maintaining the same constraints.

The first thing to notice is that it is no longer converging to the same aileron position. In this case, it finds a more outboard placement, leading to a slightly higher bending moment. In the absence of a coupling of the bending moment with the sizing process, the stress is the main constraint, as the flutter has been kept virtually the same.

Table 5: Mass optimisation via aileron resizing results (uCRM9)

	Baseline	Optima #3	Optima #4
Aileron position / span [-]	0.8	0.643	0.717
Max Mx Bending [Nm]	1.71×10^7	1.65×10^7	1.66×10^7
Structural mass [Ton]	14.702	13.055 (-11.2%)	13.034 (-11.34%)
Flutter speed [m/s]	>313	312.545	312.55
Roll capability	175.1%	186.9%	185.4%
Run time [h:min]		01:06	02:17

It is difficult to estimate whether there is a real effect on this new placement for the aileron as the results are very close. The sensitivity of the aileron placement with respect to the final mass is not that high, as shown in this case with a difference of 0.14%. And it is possible that there are discontinuities in the relation of optimal structural mass with respect to aileron position.

The big drawback with this method is the runtime; this method needs twice as much time due to the need to execute the solution 200 many more times than the previous approach, doubling the total computational cost. Within two or three full loops the first approach could converge, which meant just 2 or three executions of the solution 200, which takes the longest as it requires to run both the sensitivity analysis for structural optimisation with the flutter optimisation. For this method, the solution 200 needs to be computed around 6 to 7 times to reach convergence.

5.2 Results for high aspect ratio

Given the promising results from the uCRM9 model it is now of interest to see if it applies as well to high aspect ratio. In this section the same study will be performed but this time with the uCRM13.5 instead.

The high aspect ratio model, as anticipated, significantly increases the design process. From the beginning the model shows flutter instabilities with the baseline configuration, at around 295m/s flutter appears, as shown in figure 10.

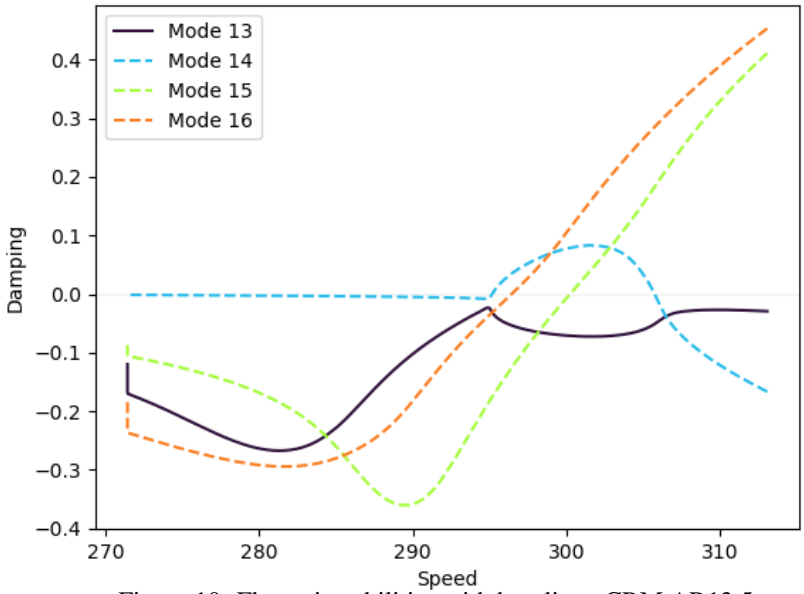

Figure 10: Flutter instabilities with baseline uCRM AR13.5

Note as well the bifurcation occurring between mode 13 and 14, as mentioned in section 2.5 this could be also one of the issues leading to the difficulty to generate a flutter-free configuration. So instead what is proposed is to use this new 295m/s target as the new constraint to be used in the MDO algorithm. The results can be seen in table 6.

Table 6: Mass - Wing bending optimisation via aileron resizing results (uCRM135)

	Baseline	Optima #1
Aileron position / span [-]	0.8	0.633
Max Mx Bending [Nm]	2.08×10^7	1.95×10^7
Structural mass [Ton]	19.312	19.303 (-0.55%)
Flutter speed [m/s]	295.17	294.7
Roll capability	179.1%	187.5%
Run time [h:min]		01:10

In this case the model is heavily constrained by flutter, structural mass reduction cannot be achieved without significant negative impacts on flutter. Only wingbox parts that have negligible effect on flutter can be optimised, this explains the minimal variation in weight.

The same happens with the second approach (see table 7), only this time the aileron placement is nowhere near the minimal bending moment optima due to a lack of sensitivity between the aileron placement and the sizing mass of the wingbox that the flutter constraint introduces. The design is extremely constrained by flutter, so that the difference in structural mass that can be achieved for different aileron positions is not big enough for the optimiser to converge to the same position.

Table 7: Mass optimisation via aileron resizing results (uCRM135)

	Baseline	Optima #2
Aileron position / span [-]	0.8	0.74
Max Mx Bending [Nm]	2.08×10^7	2.06×10^7
Structural mass [Ton]	19.312	19.304 (-0.52%)
Flutter speed [m/s]	295.17	294.7
Roll capability	179.1%	181.3%
Run time [h:min]		05:10

It is worth noting large differences in the computational times for achieving the two optima. Indeed, for the high aspect ratio model the GFEM is bigger in comparison with the short aspect ratio, which is the reason why with the second approach the difference in run time becomes much greater. It is the flutter within the sizing process which becomes a very significant computational expense.

6 CONCLUSION

Within this paper a methodology has been presented for aileron sizing through an MDO process. Starting from the base of loads optimisation and thanks to the integration of the structural sizing, there is now an insight on the potential mass savings to increase performance. In this case, more than 10% of the structural mass of the wingbox can be saved thanks to load alleviation. Two methods were proposed to solve the problem, the first one faster as it sizes the structure for minimal wing bending, and the second which will skip this step and will optimise the mass as a whole with respect to aileron position. The first method has the advantage of giving an

insight to the optimiser on how to proceed based on loads, while the second resembles more of a black box approach, with a simpler architecture as everything is contained within a single Nastran script. The study shows a significant interest to introduce the flutter discipline, given that the change of mass and stiffness induce a significant impact in the structural damping. In this case, the roll capability is not really a driver of configuration selection as both models show significant margins.

For the short aspect ratio, the model already had some headroom within flutter so it was feasible to further optimise the structure, while, on the other hand for HAR, flutter was since the beginning the main constraint. This meant that no further improvements could be reached in regard to mass, flutter instabilities are much more sensible due to the greater span and flexibility. Furthermore, the HAR model produced inconsistent results between the two methods. Flutter imposed such strict design constraints that the mass improvements were negligible for different aileron placements. This issue could be addressed by using of composite instead of metallic materials for the aeroelastic tailoring [23], an optimization of the layering to reduce weight while maintaining the rigidity of the structure. Note, however, that the models used are not the best suited for flutter analysis; thus, future work will involve the improvement of the structural models for flutter analysis.

Furthermore, since flutter turned out to be one of the main drivers of the design optimization, gust loads, which also involve dynamic aero-elastic phenomena, will be the following point to address, following studies such as [24, 25]. The aileron does not play a direct role in flutter excitation (only indirectly through structural optimisation), unlike for gust where it can alleviate the loads through a gust load alleviation function (GLA).

7 REFERENCES

[1] Handojo, V., Himisch, J., Bramsiepe, K., et al. (2022). Potential estimation of load alleviation and future technologies in reducing aircraft structural mass. *Aerospace*, 9(8). ISSN 2226-4310. doi:10.3390/aerospace9080412.

[2] Muradas Odriozola, D., Marquier, S., Morlier, J., et al. (2023). A Preliminary Low-Fidelity MDO Approach for Load Alleviation Through Movables on HAR Wing. In *Aerobest 2023*. Lisboa, Portugal: ECCOMAS, Portugal.

[3] Carrier, G. G., Arnoult, G., Fabbiane, N., et al. (2022). *Multidisciplinary analysis and design of strut-braced wing concept for medium range aircraft*. doi:10.2514/6.2022-0726.

[4] Mangalgiri, P. D. (1999). Composite materials for aerospace applications. *Bulletin of Materials Science*, 22(3), 657–664. ISSN 0973-7669. doi:10.1007/BF02749982.

[5] Bertrand, J., Fellouah, H., and Alsaif, K. (2017). Experimental evaluation of the critical flutter speed on wings of different aspect ratio. *Journal of Applied Fluid Mechanics*, 10, 1509–1514. doi:10.29252/jafm.73.245.27620.

[6] Li, Y. and Qin, N. (2022). A review of flow control for gust load alleviation. *Applied Sciences*, 12(20). ISSN 2076-3417. doi:10.3390/app122010537.

[7] Vale, J., Afonso, F., Oliveira, É., et al. (2017). An optimization study on load alleviation techniques in gliders using morphing camber. *Structural and Multidisciplinary Optimization*, 56(2), 435–453. ISSN 1615-1488. doi:10.1007/s00158-017-1673-9.

[8] ICAS (1986). *Designing a Load Alleviation System for a Modern Civil Aircraft*.

[9] EASA, Cologne, Germany (2007). *Certification Specifications for Large Aeroplanes (CS-25)*.

[10] FAA (2022). *Airworthiness Standards: Transport Category Airplanes (CFR-25)*.

[11] Brooks, T. R., Kenway, G. G., and Martins, J. R. R. A. (2019). Ucrm: undeflected common research model. doi:10.17632/gpk4zn73xn.1.

[12] NASA Common Research Model. `https://commonresearchmodel.larc.nasa.gov/`. [Accessed 07-05-2024].

[13] Brooks, T. R., Kenway, G. K. W., and Martins, J. R. R. A. (2018). Benchmark Aerostructural Models for the Study of Transonic Aircraft Wings. *AIAA Journal*, 56(7), 2840–2855. ISSN 0001-1452, 1533-385X. doi:10.2514/1.J056603.

[14] Hexagon (2021). *MSC Nastran 2022.2 Design Sensitivity and Optimization User's Guide*, 2021.4 ed.

[15] Le Lamer, Y., Morlier, J., Bénard, E., et al. (2023). Aeroelastic Analysis and Optimization of High Aspect Ratio and Strut-Braced Wings. In *AEROBEST (Thematic Conference on Multidisciplinary Design Optimization of Aerospace Systems)*. Lisbonne, Portugal.

[16] Kenway, G. K. W. and Martins, J. R. R. A. (2014). Multipoint high-fidelity aerostructural optimization of a transport aircraft configuration. *Journal of Aircraft*, 51(1), 144–160. doi:10.2514/1.C032150.

[17] Hexagon (2021). *MSC Nastran 2021.4 Aeroelastic Analysis User's Guide*, 2021.4 ed.

[18] Djojodihardjo, H. (2023). *Flutter Calculation Methods*. Singapore: Springer Nature Singapore. ISBN 978-981-16-8078-6, pp. 377–425. doi:10.1007/978-981-16-8078-6_9.

[19] Jonsson, E., Kenway, G. K., Kennedy, G., et al. (2017). *Development of Flutter Constraints for High-fidelity Aerostructural Optimization*. doi:10.2514/6.2017-4455.

[20] Jonsson, E., Mader, C. A., Kennedy, G., et al. (2019). *Computational Modeling of Flutter Constraint for High-Fidelity Aerostructural Optimization*. doi:10.2514/6.2019-2354.

[21] Gallard, F., Vanaret, C., Guénot, D., et al. (2018). Gems: A python library for automation of multidisciplinary design optimization process generation. In *2018 AIAA/ASCE/AHS/ASC Structures, Structural Dynamics, and Materials Conference*.

[22] Lambe, A. and Martins, J. (2012). Extensions to the design structure matrix for the description of multidisciplinary design, analysis, and optimization processes. *Structural and Multidisciplinary Optimization*. doi:10.1007/s00158-012-0763-y.

[23] Najmi, J., Khan, H. A., Javaid, S. S., et al. (2024). Aeroelastic tailoring for aerospace applications. *Heliyon*, 10(2), e24151. ISSN 2405-8440. doi:https://doi.org/10.1016/j.heliyon.2024.e24151.

[24] Xu, J. and Kroo, I. (2012). *Aircraft Design with Active Load Alleviation and Natural Laminar Flow*. doi:10.2514/6.2012-1428.

[25] Pusch, M., Knoblach, A., and Kier, T. (2019). Integrated optimization of control surface layout for gust load alleviation. *CEAS Aeronautical Journal*, 10(4), 1059–1069. ISSN 1869-5590. doi:10.1007/s13272-019-00367-4.

[26] Altair Engineering, Inc., Troy MI, United States (2021). *CAE Altair HyperWorks*, 2021.2 ed.

ACKNOWLEDGEMENTS

This project has been funded by the ANRT Cifre programme.

Figures containing the geometry of the uCRM aircraft, mesh plots or FEM results were achieved with Altair Hypermesh [26].

COPYRIGHT STATEMENT